



The Effect of Shielding Gas Additions on the Penetration Characteristics of Plasma-Arc Welds

For plasma processes which utilize two gas flows, a reactive gas may be added to the supplementary shield to improve penetration while the inert plasma gas protects the electrode

BY C. D. LUNDIN AND W. J. RUPRECHT

ABSTRACT. Among the more successful attempts to increase the penetration capability of the GTA process have been investigative modifications of the shielding gas. Weld studies involving reactive shielding gases such as chlorine, Freon, and sulphur hexafluoride have shown that while reactive gases enhanced penetration, they also tend to rapidly destroy the tungsten electrode.

In plasma processes, which utilize two gas flows, if an inert gas is used as the plasma gas and if the reactive gas is added to the supplementary shield, then penetration will be improved; at the same time the electrode will be protected by the inert plasma gas.

In this investigation, the penetration characteristics of welds made on two base metals—Inconel 600 and 1020 carbon steel—were evaluated as shielding gas additions of hydrogen, nitrogen, Freon-12, and Freon-14 were varied. The basis for evaluation was the resulting geometric configuration of the welds and the corresponding metallurgical characteristics.

Introduction

One of the more successful means of increasing power density, and thus the penetrating capability, of gas-shielded arc welding processes is the modification of the shielding gas. The shielding gas composition has a marked influence on the power density, arc voltage, and thermal efficiency of the welding arc.

The addition of hydrogen to argon to increase arc voltage and power density has been described by Helmbrecht and Oyler (Ref. 1) and successfully applied to plasma arc welding.

Based on paper presented at the 55th AWS Annual Meeting held in Houston, Texas, during May 6-10, 1974.

C. D. LUNDIN is Section Manager, Welding, Research & Development Division, Babcock & Wilcox Co., Alliance, Ohio, and was formerly Professor of Metallurgical Engineering, University of Tennessee, Knoxville, Tennessee; W. J. RUPRECHT is Senior Welding Engineer, ACF Industry Inc., St. Charles, Missouri.

Nestor (Ref. 2) studied the anode heat and current distribution for certain gas mixtures (argon—8.6% hydrogen; argon—17.6% nitrogen; and helium—2% argon) and found that the diatomic gas additions produced a distinct contraction of the plasma boundaries near the anode. Wilkenson and Milner (Ref. 3), in discussing heat transfer from arcs, pointed out a penetration increase resulting from the liberation of the heat of reassociation at the bottom of the weld crater.

Ludwig (Ref. 4) has shown that the difference in the weld fusion zone geometry of vacuum and inert atmosphere melted Zircaloy-2 could be attributed to a variance in anode heat output produced by a difference in the chemistry of the work-piece. Ludwig proposed that this variation in anode heat output is a consequence of a higher negative ion concentration in the arc. The source of these ions was the higher content of residual chlorine in the inert atmosphere melted Zircaloy-2. The ionization of the evolved chlorine produced a greater heat

Table 1—Operating Parameters Held Constant for the Study of the Effects of Shielding Gas Composition

Parameter	Value
Current	80 amperes (A)
Travel speed	11 ipm (4.7 mm/s)
Stand-off distance	1/8 in. (3.16 mm)
Orifice gas	Argon
Electrode	3/32 in. (2.38 mm) 2% thoriated tungsten
Copper orifice	0.118 in. (3.0 mm) diameter
Hold-down plate separation	1/2 in. (12.7 mm)
Initial plate temperature	Room temperature
Base metals	0.109 in. (2.8 mm) thick Inconel 600 and 1020 carbon steel
Electrode setback	0.068 in. (1.7 mm)

output at the anode and resulted in a deeper and narrower fusion zone.

Matchett and Frankhouser (Ref. 5) proposed that artificial additions of an electrode-negative gas (such as fluorine, chlorine, iodine, or bromine) to the weld chamber atmosphere during welding of vacuum melted Zircaloy-2 would eliminate the inherent deficiency in weld puddle geometry. Their study included the results of additions of chlorine (Cl₂), Freon-11 (CCl₃F), Freon-12 (CCl₂F₂), Freon-114 (CClF₂-CClF₂), and sulfur hexafluoride.

Matchett and Frankhouser concluded that most halogen gas additions to the argon atmosphere used in welding Zircaloy-2 resulted in an increase in the depth-to-width ratio of the weld puddle. However, at high additive concentrations (greater than 2%) the life of the tungsten electrode was adversely affected, and the weld chamber became clouded with a smoke-like reaction product. Their studies also showed that the Freon additions did not affect corrosion resistance or mechanical properties of the weld metal. Furthermore, the only effect of the additive on chemical analysis of the weld metal was to increase the chlorine content of the vacuum-melted Zircaloy to the equivalent level of that ordinarily found in inert atmosphere melted Zircaloy.

The plasma welding process utilizes two distinct gas flows; the orifice gas protects the electrode from contamination and provides the desired composition in the plasma jet, and the shielding gas provides supplementary shielding of the weld puddle. The possibility exists, therefore, that halogen gases added to the shielding gas might be aspirated into the plasma jet and be ionized outside of the plenum chamber as illustrated in Fig. 1. By operating in this manner, it should be possible to utilize the negative ion effect while maintaining the integrity of the protected tungsten electrode.

Experimental Procedure

All welds in this investigation were

made with a three phase, dc, 750 A, function controlled, magnetic amplifier type power source operated in the constant current mode. A commercially available plasma arc "add-on" control unit with a 200 A torch was used to adapt this power supply to plasma operation.

Single heats of Inconel 600 and 1020 carbon steel were used throughout this investigation to avoid heat-to-heat variations in behavior due to compositional differences. Prior to welding the sheet material was ground clean with 2/0 abrasive paper and degreased with methanol. The fixturing consisted of a copper backing plate with aluminum hold-down plates, as shown in Fig. 2. The trailing shield shown in Fig. 2 was used for all welds to protect the weld area from oxidation and contamination.

The gases used for this investigation were welding grade, bottled argon, commercial grade hydrogen and nitrogen, and refrigeration grade Freon-12 and Freon-14.

The weld depth and depth-to-width ratios were measured on polished and etched cross-sections. A minimum of three measurements were made and the average values are reported.

Mechanical tests were made with an Instron tensile testing machine. All weld metal longitudinal specimens were tested in addition to transverse specimens; included within the gage length were the fusion zone, the heat-affected zone, and base metal.

The current and voltage levels were monitored by both pen-type recorders

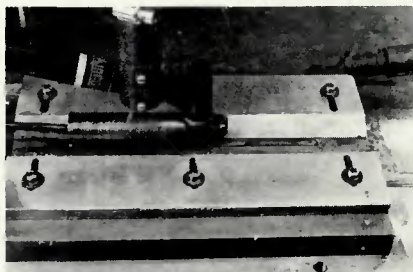


Fig. 2—Torch, trailing shield and hold-down fixture

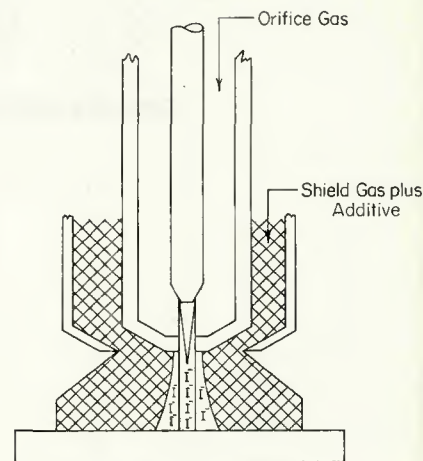


Fig. 1—Schematic illustration of the method of introducing the shielding gas additive

and by photographs of oscillographic displays where appropriate.

In order to properly identify the effect of varying the shielding gas composition, it was necessary to maintain most of the weld parameters constant. For this investigation the variables were shielding gas composition and orifice gas flow rate. The values of the fixed parameters are listed in Table 1.

Results and Discussion

For this investigation, weld penetration and depth-to-width ratio were selected to characterize the effect of shielding gas additions. Unless stated otherwise, the results discussed are for the Inconel 600 alloy base metal.

Figure 3 illustrates the relationship between weld penetration, shielding gas composition, and orifice gas flow rate at constant current. Two curves show the effect of 10% and 15% additions of hydrogen to the argon shielding gas. A curve for a 100% argon shielding gas is included in Fig. 3 as a reference. Figure 3 shows that an increase in penetration results from an increase in the percentage of hydrogen in the shielding gas. Figure 3 also shows that weld penetration for both hydrogen additions reaches a minimum at an orifice gas flow rate of 2.5 cfh (70.8 litres/h).

Figure 4 shows the effect of an addition of nitrogen to the shielding gas. The reference curve for 100% argon shielding gas illustrates the increase in penetration that is achieved with nitrogen additions to the shielding gas. It should be noted that weld penetration for nitrogen addition to the shielding gas has a maximum at an orifice gas flow rate of 3.5 cfh (99 litres/h). Work with nitrogen additions was not extended beyond 15% N₂ because a further increase in the N₂ percentage did not significantly improve the penetration.

The relationship between depth-to-width ratio and orifice gas flow rate for additions of hydrogen and nitrogen is shown in Figs. 5 and 6 respectively. The arc current is constant at 80 A. The depth-to-width ratio in Fig. 5 is lowest at an orifice gas flow rate of 2.5 cfh (70.8 litres/h), as is penetration in Fig. 3. Similarly, the depth-to-width ratio in Fig. 6 is greatest at an orifice gas flow rate of 3.5 cfh (99 litres/h), as is penetration in Fig. 4. It should be noted, however, that the hydrogen addition is more effective at low and high orifice gas flow rates than at intermediate flow rates. The converse appears to be true for nitrogen additions.

The increased penetration that results from the diatomic gas additions cannot be related to increased arc voltages alone. The maximum arc voltage increase for any hydrogen or nitrogen additions was 2 volts or V (e.g., an arc voltage of 15 V for argon, vs. 17 V for argon and additions). The 2 V increase would only produce an increase of 10% in the energy input:

$$E.I. = 60 \frac{\text{(Voltage} \times \text{Amperes)}}{\text{Travel Speed (in ipm)}} \quad (1)$$

whereas the increase in material melted with additives is approximately 50%, and the penetration is increased by as much as 160%.

The increase in penetration may be related in part to the phenomena noted by Okada and Maruo (Ref. 14) that, when the mixed gases were used with the GTA process, the heat loss decreased with increasing content of hydrogen or nitrogen—also, that the action of the dissociated gas as a carrier of electrical energy increases the thermal efficiency of the plasma jet. It may be these two effects, the increase in thermal efficiency and the addition of recombination energy to the anode surface, which primarily account for the increased penetration. The shapes of the curves are not amenable to explanations consistent with current theories.

Ludwig (Ref. 4) reported a difference in penetration in gas tungsten-arc welds in zirconium due to trace impurities either in or on the surface of the material. He attributed the increased penetration to chlorine emanating from the weld pool, attaching electrons, and forming negative ions, thereby increasing the negative space charge and the potential drop, and thus increasing heat input at the anode. Ludwig suggests that electronegative materials such as the halogens would be expected to increase the anode heat input.

Following this suggestion this investigation was based on the idea that an increase in penetration could be achieved by the artificial doping of halogens in the welding arc by the

addition of either Freon-12 or Freon-14 to the argon shielding gas. Freon gases were chosen for this study because they are non-toxic and non-reactive until they enter the arc. Chlorine and fluorine gases, on the other hand, are highly toxic and highly reactive even at room temperature. Therefore, the applicability of the pure gases would be limited.

Figure 7 shows the relationship between weld penetration and orifice gas flow rate for various percent additions of Freon-12 to the shielding gas. Figure 8 shows the same relationship for Freon-14 additions. A curve for the same 80 A arc operating in pure argon is also included in Figs. 7 and 8 as a reference to illustrate the increased penetration obtained with the Freon gas additions.

Figures 7 and 8 show that the weld penetration was increased by the addition of Freon-12 or Freon-14. However, the electronegative ion theory predicted greater penetration increases for the more electronegative material. Thus Freon-14 with a chemical composition CF_4 should have been more effective than Freon-12 with composi-

tion CCl_2F_2 . Figures 7 and 8, however, show that instead it was the Freon-12 additions which had the greater effect on the penetration. This may be explained by the fact that the electronegative materials—chlorine and fluorine—were introduced into the arc as compounds. Thus, the effect of either CF_4 or CCl_2F_2 may depend on the degree of compound dissociation in the arc.

Because of the lack of thermochemical data for CCl_2F_2 , the relative tendency for dissociation was estimated by a comparison of the empirical bonding contributions of chlorine and fluorine to the free energy of compound formation. From this empirical method it was determined that the negative free energy of formation was greater for CF_4 than CCl_2F_2 . Therefore, a greater energy would be needed to dissociate CF_4 than CCl_2F_2 .

Based upon this low temperature empirical determination is the idea that the same trend may hold true for the dissociation of the compounds in a high temperature welding arc. Thus, the degree of dissociation in the arc would be greater for CCl_2F_2 (Freon-12)

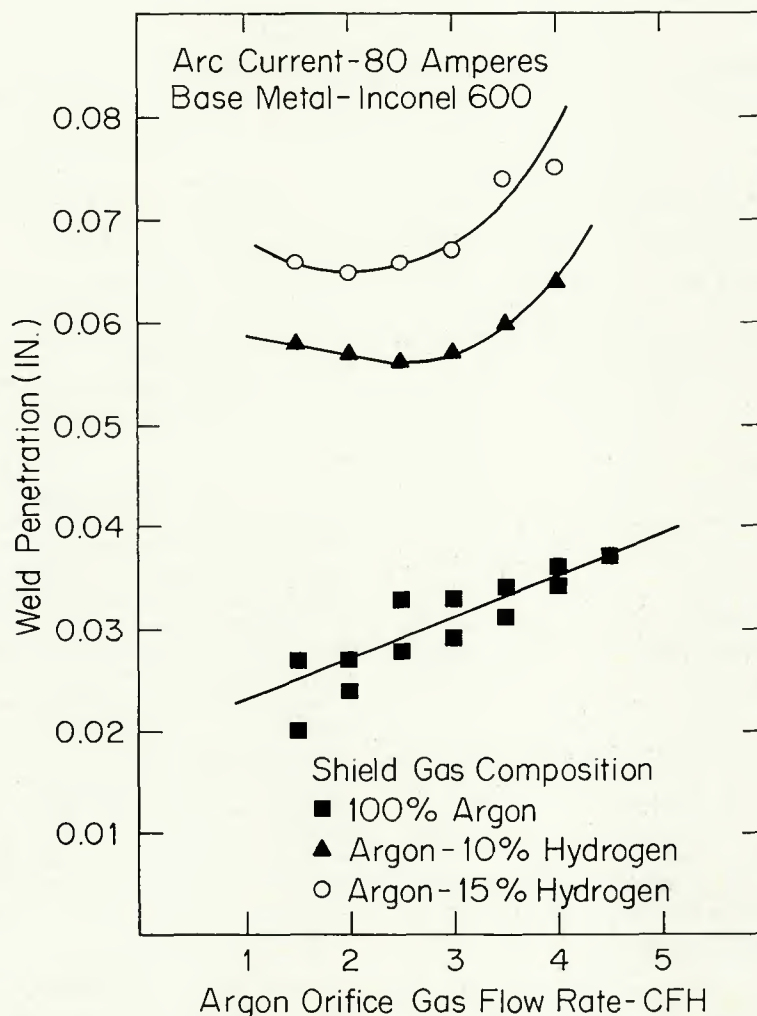


Fig. 3—Effect of orifice gas flow rate on weld penetration with hydrogen additions to the shield

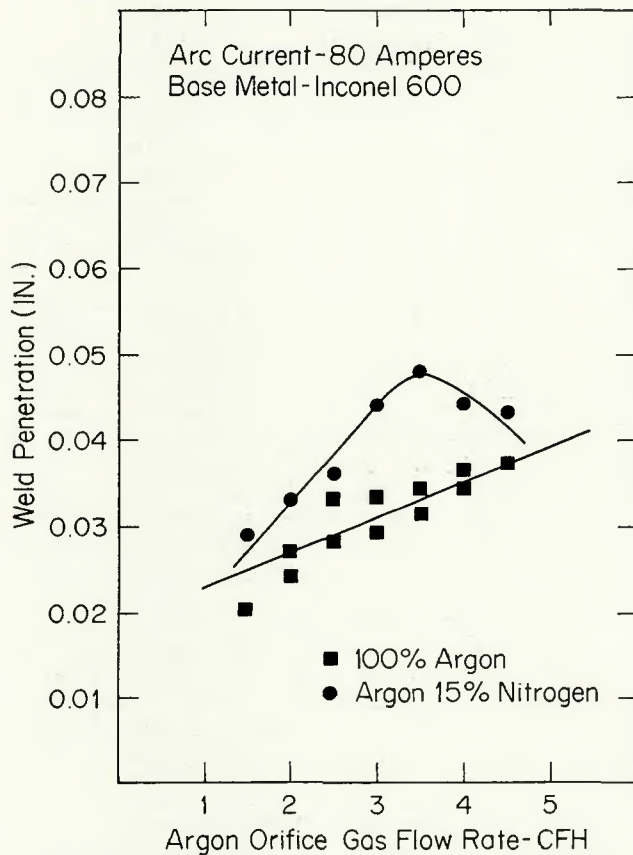


Fig. 4—Effect of orifice gas flow rate on weld penetration with nitrogen additions to the shield

than for CF_4 (Freon-14). It would follow then that the electronegative ion effect would be greater for Freon-12. This conclusion may be drawn from a comparison of Figs. 7 and 8.

The curves presented for the Freon additions to the shielding gas show characteristic maxima at an orifice gas flow rate of 2.5 cfh (70.8 litres/h). The corresponding depth-to-width ratios show the same behavior with a maximum value also occurring at an orifice gas flow rate of 2.5 cfh (70.8 litres/h).

The peak in the curves is attributed to the manner in which the gas addition enters the arc, and to the increased orifice gas flow rates. The plasma torch has two separate gas flows: the orifice gas, and the shielding gas. As has been stated, the additions which react in the arc are added to the shielding gas, and not the orifice gas which forms the arc.

The additions are introduced into the arc by an aspiration effect produced by the interaction of the high velocity orifice gas and the slow moving shielding gas. In addition, the arc pressure increases with increasing orifice gas flow rate. From the peak in the curve it appears that at an orifice gas flow rate of 2.5 cfh (70.8 litres/h) and greater, the high velocity arc stream acts as a balance against the aspiration effect, thereby decreasing the amount of gas additive that enters

the arc.

Another consideration is that an increase in the volume of gas in the arc occurs with increasing orifice gas flow rate and tends to lower the concentration of the additive in the arc. These two effects, a decrease in the amount of additive entering the arc by aspiration, and the dilution produced by higher relative flow rates, would account for the sharp drop in penetration for increasing orifice gas flow rates in excess of 2.5 cfh (70.8 litres/h).

The arc voltages which were recorded for the welds made with Freon gas additives to the shielding gas varied by less than 3 V from those welds made without additions. Freon-12 caused the greatest increase in arc voltage (18 vs. 15 V). If this increase in arc voltage is assumed to be evenly distributed along the arc length, as in energy input equation (1) the increase in energy input produced by an increase in arc voltage of three volts is approximately 20%. This would not account for the observed increase in penetration and in volume of metal melted per unit length of weld that occurred when either Freon-12 or Freon-14 was added to the shielding gas.

The maximum increase in penetration was 180% compared to the pure argon weld, and the cross sectional area of the weld metal was at least 100% greater in all cases for the Freon

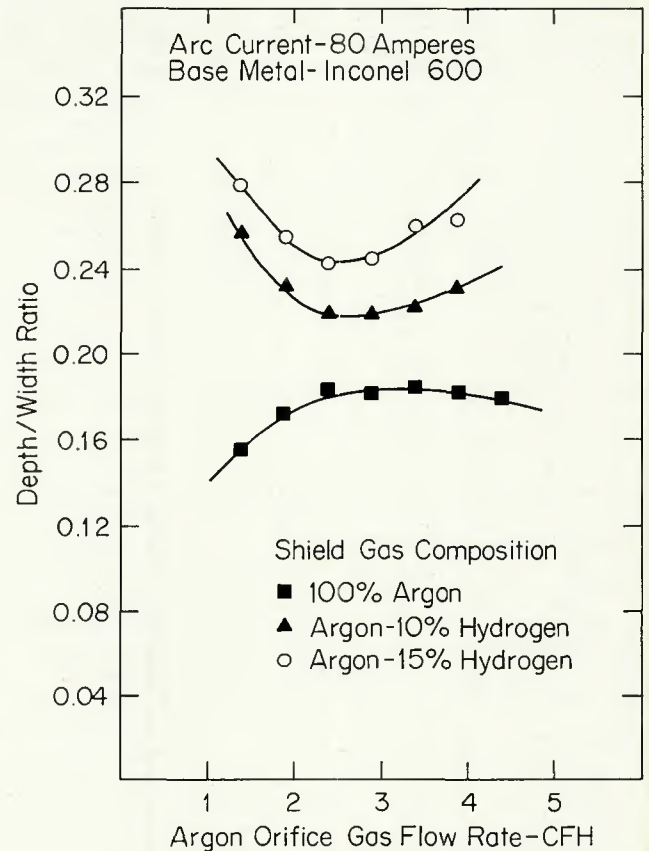


Fig. 5—Effect of orifice gas flow rate on depth/width ratio with hydrogen additions to the shield

additive welds. If, however, the 3 V increase occurs in the anode drop region only, as Ludwig has postulated, a significant increase in penetration and melting efficiency would occur.

The system used to record the arc voltage did not have the capability of separately identifying the voltage contribution of the anode drop, cathode drop and plasma regions. Direct measurements of this sort are difficult to make without serious perturbation of the welding arc and were not attempted in this investigation. Thus, the mechanism of the negative ion interaction in the welding arc could not be precisely determined in this investigation.

In order to determine if the effects of additions to the shielding gas are dependent on the base metal, a check was made using a plain carbon steel base metal instead of Inconel 600. The 1020 steel was ground to the same thickness as the Inconel 600 and prepared for welding in the same manner. Freon-12 and Freon-14 were used for this check since hydrogen and nitrogen would have had a deleterious effect on the fusion and heat-affected zones. The arc current and percent addition of Freon in the shield were the same as for the Inconel 600 test welds.

A comparison of the results obtained for Inconel 600 and plain carbon steel can be made by reference

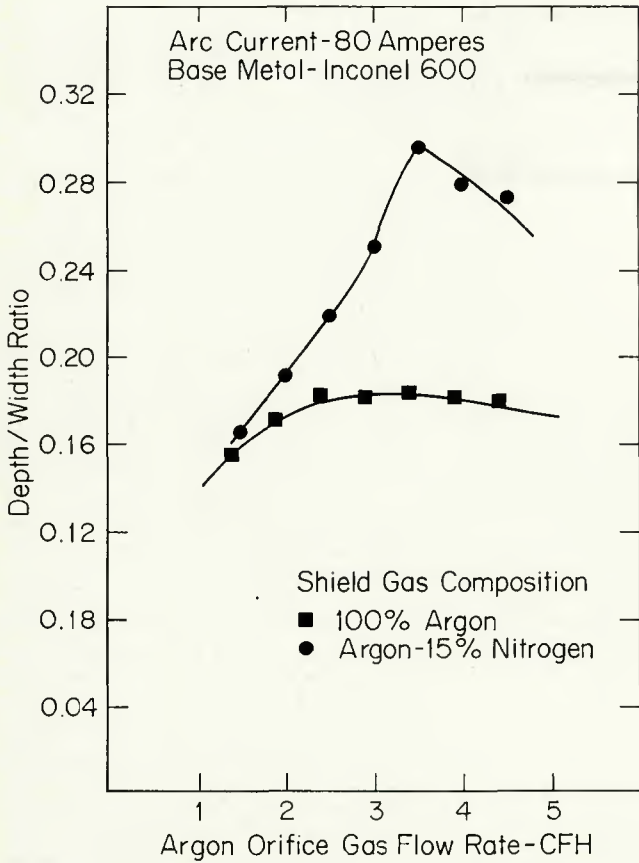


Fig. 6—Effect of orifice gas flow rate on depth/width ratio with nitrogen additions to the shield

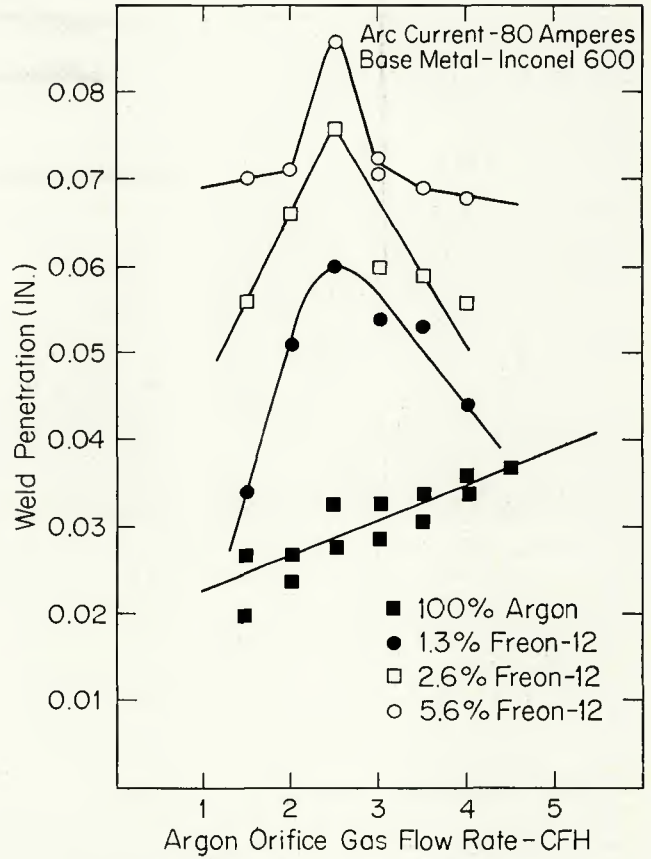


Fig. 7—Effect of orifice gas flow rate on penetration with Freon-12 additions to the shield

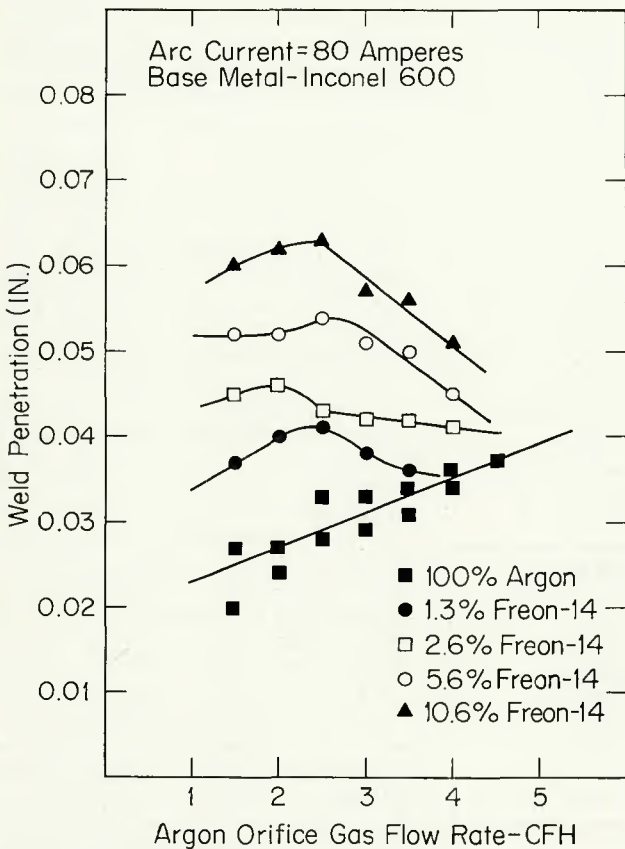


Fig. 8—Effect of orifice gas flow rate on penetration with Freon-14 additions to the shield

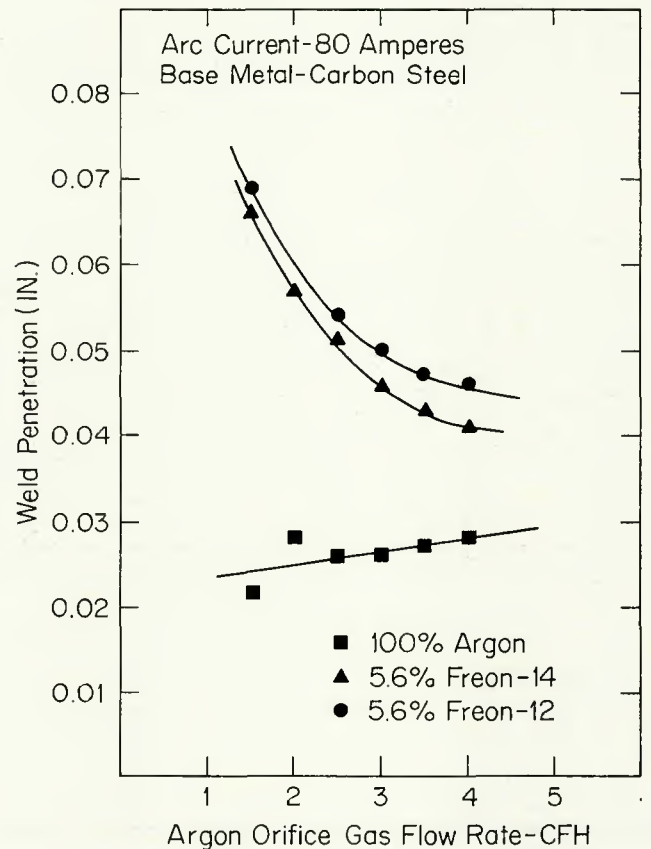


Fig. 9—Effect of orifice gas flow rate on penetration with Freon-12 and Freon-14 additions to the shield. (Carbon steel base metal)

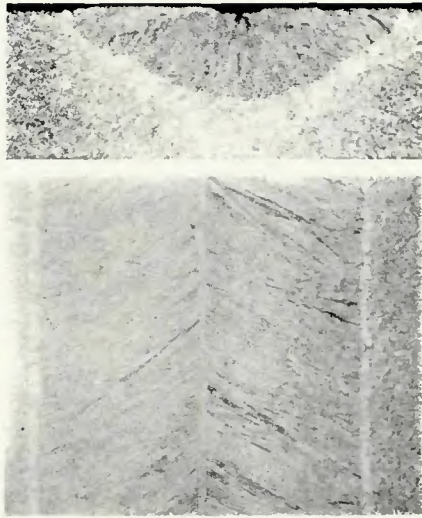


Fig. 10—Fusion zone microstructure of an 80 A partial penetration weld, with hydrogen shield addition: A (top)—transverse section; B (bottom)—section parallel to and in the plane of the top surface of the sheet. WAZAU's reagent. X12½ (reduced 47% on reproduction)

to Figs. 7, 8, and 9. These show penetration as a function of orifice gas flow rate for pure argon and argon plus Freon-12 and Freon-14 at an arc current of 80 A and a travel speed of 11 ipm (4.7 mm/s).

The differences in penetration for the pure argon welds are rather insignificant since the data are practically identical, especially at low flow rates. The penetration curves for the Freon additions are quite different, however, with the Freon-carbon steel welds exhibiting the greatest penetration at the lowest orifice gas flow rate and a decrease in penetration with increasing orifice gas flow rate. Also, the Freon-12 and Freon-14 curves for carbon steel are quite similar in penetration magnitude. There is no peak in the penetration curves at intermediate flow rates as with the Inconel 600 alloy; however, the same total penetration can be achieved for both materials but at different orifice gas flow rates.

The melting points and specific heats of the carbon steel and Inconel 600 are virtually identical, and the

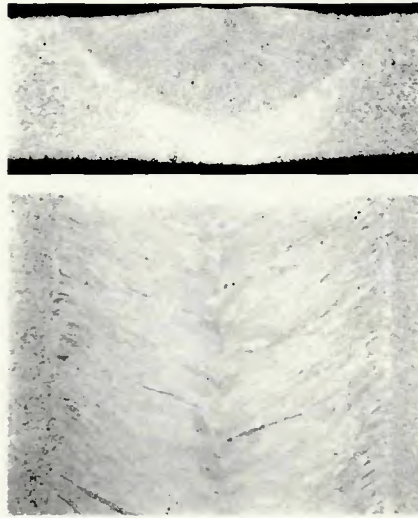


Fig. 11—Fusion zone microstructure of an 80 A partial penetration weld with Freon-12 shield addition: A (top)—transverse section; B (bottom)—section parallel to and in the plane of the top surface of the sheet. WAZAU's reagent. X12½ (reduced 50% on reproduction)

difference in arc voltage for the welds on the two materials was less than 1 V. Although no surface tension data exist for the specific alloys, the surface tensions reported for pure iron and pure nickel reveal a difference of only 5%. This does not at first appear significant. However, the influence of gas additives on the surface tension is unknown.

The only significant physical property difference is the thermal conductivity with the conductivity of steel being three times that of Inconel 600. This difference in conductivity does not manifest itself in the pure argon welds, so it would not be expected to be any more effective with the gas additions.

The experimental evidence in this portion of the investigation strongly suggests that the shielding gas addition may interact with the surface of the molten weld pool and affect the surface tension of the liquid pool. The arc cratering effect is thereby altered, and consequently the penetration is influenced, thus causing the difference in the shielding gas additive

effect noted.

The following general results were noted for the addition of either hydrogen, nitrogen, Freon-12 or Freon-14 to the argon shielding gas:

1. There was an increase in penetration with the addition of each gas.
2. For each gas the increase in penetration was proportional to the increase in the percentage of gas added.
3. The effect of Freon additions is partially dependent on the base material.
4. Use of Freon-12 in the shielding gas resulted in some erosion of the outer surface of the copper orifice. Freon-14 had no detectable effect on the copper orifice; the tungsten electrode remained free of contamination and erosion.

In addition to the above, it was noted that a fine powder formed on the test sheets when Freon additions were used in the shielding gas. X-ray analysis of the powder formed on the Inconel sheet using an Ortec 78000 Series X-ray Energy Analysis system with an AMR 900 scanning electron microscopy indicated that the powder contained nickel, chromium, manganese, iron, copper, and barium. Using a Debye-Scherrer powder pattern and the three lines of highest intensity method, it was determined that the predominant component of the powder produced by Freon-12 additions was an iron-chlorine compound Fe_3Cl ; the powder produced by Freon-14 additions contained a chromium-fluorine compound, CrF_3 .

The formation of Fe_3Cl or CrF_3 when Freons were added to the shielding gas indicates there is an interaction between the gas addition and the base material. Also, the fact that CrF_3 was not formed for the Freon-12 additive indicates that chlorine is the more reactive component when both chlorine and fluorine are present.

A metallographic study of the fusion zone and heat-affected zone of the Inconel 600 welds was performed to determine the relationship between shielding gas additions and microstructural features. A comparison of the sections obtained parallel to and in the plane of the sheet surface reveals two different grain growth patterns for welds made with the same welding parameters—Figs. 10 and 11.

Figure 10 shows elongated grains which extend to the weld center line, while Fig. 11 shows that the elongated grains extend approximately one-third of the way into the fusion zone and then the grain growth direction changes, as evidenced by the elliptically-shaped grains. The weld in Fig. 10 was made using a shielding gas

Table 2—Tensile Data^(a) for the Selected Welds and the Inconel 600 Base Material

Weld designation	0.2% offset yield strength, psi ^(b)	Ultimate tensile strength, psi ^(b)	Percent elongation ^{(b)(c)}
Hydrogen addition	46,200 L	84,500 L	30.8 L
	45,600 T	87,900 T	23 T
Freon-12 addition	49,300 L	88,700 L	29.6 L
	48,900 T	88,200 T	23.4 T
Base material	37,400	93,000	42.5

(a) All data represent the average of three separate tests.

(b) L—tensile axis parallel to weld direction, longitudinal direction; T—tensile axis normal to weld direction, transverse direction.

(c) 2 in. gage length.

composition of 85% argon—15% hydrogen; the gas composition for the weld shown in Fig. 11 was 89.4% argon—10.6% Freon-12.

The explanation for the variation in grain orientation in the partial penetration melt-in welds made with the hydrogen and Freon-12 shielding gas additions is not readily apparent from the weld pool configurations exhibited. The penetration for the Freon-12 weld was greater than that for the hydrogen weld and, all else being equal, should have had a greater tendency than the hydrogen weld toward producing growth parallel to the sheet surface. Thus, the Freon-12 addition may have a controlling influence.

Mechanical tensile tests of these two partial penetration welds showed that the yield strength of the autogenously welded fusion zones were 22 to 32% higher than the as-received base metal, while the ultimate tensile strength was 5 to 9% lower. The data for these two welds are shown in Table

2. It can be seen that the more random grain orientation of the weld made with Freon-12 shielding gas additions resulted in higher values of the mechanical properties.

Conclusion

The results of this investigation have shown that, because of the two separate gas flows of the plasma process (an orifice gas and a shielding gas), gas additives such as Freon-12 (which destroy the electrode in GTA welding when they enter the arc near the electrode) can be added to the shielding gas of the plasma torch and enter the arc away from the electrode.

It is also demonstrated that the effect of shielding gas composition on plasma arc weld penetration is dependent on the shielding gas additive, the orifice gas flow rate, and the base metal.

The effect of the various shielding gas additives appears to be related to a complex interaction influencing the

anode drop, weld pool surface tension and the arc cratering effect. Information obtained in a recently completed study of weld pool geometry suggests that the anode drop alteration is the most influential.

References

1. Helmbrecht, W. H., and Oyler, G. W., "Shielding Gases for Inert-Gas Welding," *Welding Journal*, 36(10), Oct. 1957, pp. 969 to 979.
2. Nestro, O. H., *Physics of the Welding Arc*, A Symposium organized by the Institute of Welding, London, October 29-November 2, 1962.
3. Wilkenson, J. B., and Milner, D. R., Heat Transfer From Arcs, *British Welding Journal*, Vol. 7, No. 2, February, 1960, pp. 115-128.
4. Ludwig, H. C., "Arc Welding of Vacuum and Inert-Atmosphere Melted Zircaloy-2," *Welding Journal*, 36(7), July 1957, Research Suppl., 335-s to 341-s.
5. Matchett, R. L., and Frankhouser, W. L., *Halogen Additions to Inert-Atmosphere Weld Chambers*, AEC Report, Contract AT-11-1 GEN-14, May, 1960.

AWS D10.10-75 Local Heat Treatment of Welds in Piping and Tubing

In the manufacture of welded articles or structures in the shop or in the field, it may be desirable, for a variety of reasons, to heat the weld regions before welding (preheating), between passes (interpass heating), or after welding (postheating). This document presents in detail the various means commercially available for heating pipe welds locally, either before or after welding, or between passes. The relative advantages and disadvantages of each method are also discussed. Although the document is oriented principally toward the heating of welds in piping and tubing, the discussion of the various heating methods is applicable to any type of welded fabrication.

Topics covered include the following:

- Measurement of Temperature
- Induction Heating
- Electric Resistance Heating
- Flame Heating
- Exothermic Heating
- Gas-Flame Generated Infrared Heating
- Radiant Heating by Quartz Lamps.

The price of AWS D10.10-75, Local Heat Treatment of Welds in Piping and Tubing, is \$3.50. Discounts: 25% to A and B members; 20% to bookstores, public libraries and schools; 15% to C and D members. Send your orders to the American Welding Society, 2501 N.W. 7th Street, Miami, FL 33125. Florida residents add 4% sales tax.